약학석사학위논문

Anti-leukemic properties of aplysinopsin derivative EE-84 alone and in combination with BH3 mimetic A-1210477

Aplysinopsin 유사체 EE-84의 항 백혈병 특성 및 BH3 모방체 A-1210477와의 동반상승효과 연구

2020년 2월

서울대학교 대학원

약학과 의약생명과학전공

김 수 아

ABSTRACT

Anti-leukemic properties of aplysinopsin derivative EE-84 alone and in combination with BH3 mimetic A-1210477

Su A Kim

College of Pharmacy

The Graduate School

Seoul National University

Aplysinopsins are a class of marine indole alkaloids that exhibit a wide range of biological activities such as prevention of neoplastic growth on an array of different cancer cell lines. Although both the indole and N-benzyl moieties of aplysinopsins are known to possess anti-proliferative activity against cancer cells, their mechanism of action remains unclear. Through *in vitro* and *in vivo* proliferation and viability screening of newly synthesized aplysinopsin analogs on myelogenous leukemia cell lines and zebrafish toxicity tests as well as analysis of differential toxicity in non-cancerous RPMI 1788 cells, EE-84 was identified as a promising novel drug candidate against myeloid leukemia. This indole derivative demonstrated drug-likeness in agreement with Lipinski's rule of five and was responsible for cell cycle dysregulation in K562 cells in line with its cytostatic effect. EE-84-treated K562 cells likewise underwent morphological changes suggesting mitochondrial dysfunction. Finally, the synergistic cytotoxic effect of EE-84 with a BH3 mimetic, the Mcl-1 inhibitor, A-1210477, against K562 cells was demonstrated, highlighting the inhibition of anti-apoptotic Bcl-2 proteins as a promising therapeutic approach against myeloid leukemia in combination with EE-84.

Keywords : aplysinopsin analogs; indole alkaloids; marine source; chronic myeloid leukemia; BH3 mimetics

Student Number : 2018-27766

ABBREVIATIONS

AML	**Acute myeloid leukemia**
Bcl-xL	**B-cell lymphoma extra large**
Bcr-Abl	**Breakpoint cluster region-Abelson**
BH	**Bcl-2 homology domain**
BSA	**Bovine serum albumin**
CCyR	**Complete cytogenetic response**
CFA	**Colony formation assay**
CML	**Chronic myeloid leukemia**
DMSO	**Dimethyl sulfoxide**
FBS	**Fetal bovine serum**
FDA	**Food and Drug Administration**
FLT3	**FMS-like tyrosine kinase 3**
GI	**Growth inhibition**
HPF	**Hours post fertilization**
IC	**Inhibitory concentration**
ITD	**Internal tandem duplication**
LogP	**Octanol-water partition coefficient**
MPER	**Mammalian protein extraction reagent**
Mcl-1	**Myeloid cell leukemia 1**
MTT	**3-(4,5-dimethylthiazol-2-l)-2,5,-diphenyltetrazolium bromide**
PARP-1	**Poly (ADP-ribose) polymerase**
PBS	**Phosphate buffered saline**
PI	**Propidium iodide**
PMSF	**Phenylmethylsulphonyl fluoride**
PTU	**Phenylthiourea**
RPMI	**Roswell Park Memorial Institute**

SA	**Surface area**
SD	**Standard deviation**
SDS-PAGE	**Sodium dodecyl sulfate polyacrylamide gel electrophoresis**
TKD	**Tyrosine kinase domain**

Table of Contents

1. INTRODUCTION

For many years, researchers struggled to find effective cures to treat leukemia, a malignancy of the blood or bone marrow. Two types of leukemia, acute myelogenous leukemia (AML) and chronic myelogenous leukemia (CML), in particular, pose tough challenges to physicians as there is no absolute cure for these two diseases.

AML, a group of neoplasms that originate from precursor cells committed to the myeloid cell-line differentiation, is a disease that is characterized by genetic and epigenetic heterogeneity and poor prognosis [1]. AML shows a 5-year overall survival rate of 40%-45% in the young and less than 10% in the elderly (>60 years of age). Despite the fact that a high percentage of patients undergo complete remission after chemotherapy, the majority of them relapse within 3 years [2]. The FMS-like tyrosine kinase 3 – internal tandem duplication (FLT3-ITD) and FLT3-TKD (tyrosine kinase domain) mutations are biomarkers for high risk AML, and FLT3 inhibitors such as midostaurin and gilteritinib, recently approved by FDA, have shown promising therapeutic results in the treatment of AML patients [3]. However, drug resistance, set of side effects, and high risk of relapse highlights the need for novel treatments as those diagnosed with AML often result in fatal outcomes.

CML is a disorder that is driven by the expression of the oncogenic hybrid gene *BCR-ABL1*, which codes for a leukemogenic tyrosine kinase [4]. Since the discovery of imatinib, a tyrosine kinase inhibitor (TKI), the overall survival rate of patients with CML have drastically increased. Imatinib as first-line therapy selectively inhibits the BCR-ABL fusion protein activity, and is proven to achieve durable responses in patients [5]. Cancer cells develop multiple mechanisms to escape chemotherapy. Therefore, despite the high remission rate, a significant number of patients develop resistance or are intolerant to imatinib treatment. In fact, 33% of patients who have received imatinib treatment do not achieve a complete cytogenetic response (CCyR) [6].

Aplysinopsin and its derivatives possess rich structural diversity, and have been reported to exhibit a wide range of medicinal and biological activities, ranging from

neuromodulation [7], antineoplastic [7], antiplasmodial [8] to antimicrobial activities [9]. Neuromodulatory activities have attracted the most interest in aplysinopsins' bioactivity as they have been found to act on both the serotonin receptor and the monoamine oxidase system [8]. Moreover, aplysinopsins displayed cytotoxicity against a range of cancer cell lines [10]. However, their anticancer potential in leukemic cell lines, as well as their corresponding molecular mechanisms remain to be investigated in detail.

In this study, the anti-leukemic activity of aplysinopsin (EE-115) and several of its analogs EE-31, EE-80, EE-84, EE-92, and EE-118 (Scheme 1) was evaluated in the AML U937 and CML K562 cell lines. Out of the aplysinopsin derivatives examined, EE-84 was identified as a promising drug lead as it exhibited drug-like properties in line with Lipinski's rule of five and showed differential toxicity in leukemia cells in comparison to a non-cancerous cell line RPMI 1788. It also displayed non-toxic effects *in vivo* on zebrafish. Furthermore, EE-84 showed cytostatic activity in agreement with cell cycle dysregulation. Moreover, EE-84 sensitized CML K562 cells against the Mcl-1 inhibitor, A-12101477, to induce caspase-dependent apoptosis. Altogether, this study provides basis for further studies of the aplysinopsin analog EE-84 as a preclinical drug candidate against leukemia.

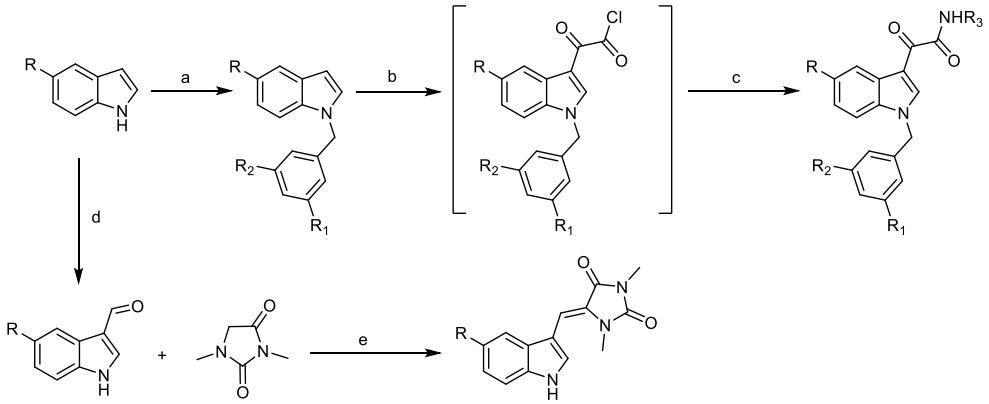

Scheme 1. Synthetic pathway for preparation of aplysinopsin EE-115 and its analogs EE-31, EE-80, EE-84, EE-92, and EE-118. Reagents and conditions: a) benzyl chlorides, NAH, DMF; b) oxalyl chloride, dry ethyl ether, heating; c) the reactant amines 2-cyanoacetohydrazide and 1-(2-amino-5-methyl-4,5,6,7-tetrahydrobenzo[b]thiophen-3-yl)ethan-1-one, dry THF, TEA, stirring, 3h; d) $POCl_3$ DMF, 0°C, NaOH; e) piperidine, reflux, 4h. The aplysinopsin compounds were synthesized and provided by Eslam R El-Sawy, PhD, Chemistry Department of Natural Compounds, National Research Centre, 12622 Dokki, Giza, Egypt.

2. MATERIALS AND METHODS

2.1. Chemistry

All reagents and solvents were of commercial grade. Melting points were determined on the digital melting point apparatus (Electro thermal 9100, Electro thermal Engineering Ltd, serial No. 8694, Rochford, United Kingdom) and were uncorrected. Elemental analyses were performed on CHNS-O analyzer (Perkin-Elmer, USA) and were found within ± 0.4 % of the theoretical values. ^{1}H and ^{13}C NMR spectra were measured with a Bruker Avance spectrometer (Bruker, Germany) at 400 and 101 MHz, respectively, using TMS as the internal standard. Hydrogen coupling patterns are described as (s) singlet, (d) doublet, (t) triplet, (q) quartet and (m) multiplet. The chemical shifts were defined as parts per million (ppm) relative to the solvent peak. The reaction progress was checked by pre-coated TLC Silica gel 0.2 nm F254 nm [Fluka], visualized under UV lamp 254 & 365 nm. 2-Cyanoacetohydrazide [37]; N-benzyl indoles [38] methyl creatinine [39]; 5-bromo and 5-methoxy indole-3-aldehyde [40] were prepared as reported. 1-(2-Amino-5-methyl-4,5,6,7- tetrahydrobenzo[b]thiophen-3-yl)ethan-1-one [41] was provided by Ahmed B. Abdelwahab, PhD, UMR CNRS 7565 SRSMC, Université de Lorraine, 57070 Metz, France. The aplysinopsin compounds was synthesized and provided by Eslam R El-Sawy, PhD, Chemistry Department of Natural Compounds, National Research Centre, 12622 Dokki, Giza, Egypt.

2.2. Cell Lines and Cell Cultures

The human histiocytic lymphoma U937, human chronic myeloid leukemia K562 (ATCC, Manassas, USA), and the normal B lymphocyte RPMI 1788 cell lines (KCLB, Seoul, South Korea) were cultured in Roswell Park Memorial Institute (RPMI) 1640 medium (Lonza, Basel, Switzerland), supplemented with 10% heat-inactivated fetal bovine serum (FBS) (Biowest, Riverside, USA) and 1% penicillin-streptomycin solution (100X) (GenDEPOT, Katy, USA). Cells were maintained at 37°C and 5% of CO2 in a humified atmosphere. Mycoplasma detection by

MycoalertTM (Lonza) was performed every 30 days and cells were used within 3 months after thawing.

2.3 Compounds

Mcl-1 inhibitor, A-1210477 (S7790, Selleckchem, USA) was used in single and combination treatments. Etoposide (E1383, Sigma-Aldrich, USA), Imatinib (SML 1027, Sigma-Aldrich, USA), and Celecoxib (PZ0008, Sigma-Aldrich, USA) were used as positive controls. Caspase inhibitor 1 (z-VAD-fmk, 187389-52-2, Calbiochem, USA) served for the inhibition of caspase-dependent apoptosis.

2.4. Cell Proliferation and Viability

Cell proliferation and viability were assessed by the trypan blue exclusion method (Lonza) and viable cells were counted using a hematocytometer (Marienfield, Lauda- Königshofen, Germany). Differential toxicity was calculated by comparing the viability of RPMI 1788 cells to the viability of cancer cells (normal/cancer cells). The difference in viability was expressed in terms of fold change.

2.5. Colony Formation Assay

For colony formation assays, 1000 cells were grown in a semisolid methylcellulose medium (Methocult H4230, StemCell Technologies Inc., Vancouver, Canada) supplemented with 10% FBS and indicated concentrations of compound. Colonies were detected after 10 days of culture by adding 1mg/mL of 3-(4,5-dimethylthiazol-2-yl)-2,5-diphenyltetrazolium bromide (MTT) reagent (Sigma-Aldrich) and were analyzed by Image J 1.8.0 software (U.S. National Institute of Health, Bethesda, MD, USA).

2.6. Quantification of Apoptosis and Necrosis

The percentage of apoptotic cells was quantified as the fraction of cells showing fragmented nuclei, as assessed by florescence microscopy (Nikon, Tokyo, Japan) after staining with Hoechst 33342 (Sigma-Aldrich) and propidium iodide (Sigma-Aldrich).

2.7. In silico Drug Likeliness Properties

Lipinski's 'rule of five' for drug likeliness properties was evaluated using the SCFBio website [http://www.scfbio-iitd.res.in/].

2.8. Zebrafish Toxicity

For toxicity assays, embryos were treated with 0.003% phenylthiourea (PTU) 14 h before the assay to remove pigmentation. 2 h before the assay, the embryo's shell was eliminated and then treated for up to 24 h with aplysinopsin compounds at indicated concentrations in 24-well plates. Viability and abnormal development were assessed after 24 h of treatment under light microscopy (Carl Zeiss Stereo microscope DV4, Seoul, Korea). Pictures were taken by fixing embryos onto a glass slide with 3% methylcellulose (Sigma-Aldrich).

2.9. Cell Cycle Analysis

Cells were collected and fixed in 70% ethanol. DNA was stained with propidium iodide (PI) solution (1 µg/mL, Sigma-Aldrich, St. Louis, USA) in 1XPBS (Biosesang, Seongnam, South Korea), supplemented with RNase A (100 µg/mL, Roche, Basel, Switzerland). Samples were analyzed by flow cytometry using the FACSCalibur™ system, Becton Dickinson (BD) Biosciences (San Jose, CA, USA). Data were recorded statistically (10000 events/sample) using the Cell Quest software (BD Biosciences) and analyzed using Flow-Jo 8.8.5 software (Tree Star, Inc, Ashland, OR, USA).

2.10. Cell Morphology / Wright-Giemsa Staining

Diff Quik staining was used to analyze the morphological features of compound-treated cells. Approximately $3x10^5$ cells were seeded in each well of a 24-well plate and treated with EE-84 at the indicated concentrations for indicated hours of interest. Cells were then spun onto a microscope glass slide for 5 minutes at 500g using a cytopad with caps (Elitech Group Inc, Puteaux, France). Cells were fixed, air-dried, and then stained with the Diff-Quik staining kit (Sysmex, Kobe, Japan). The stained cells were examined, and images were captured with an inverted microscope (Nikon Eclipse Ti2).

2.11. Flow cytometry acquisition and analysis

Flow cytometry acquisitions were performed on FACSCalibur™ (BD Biosciences) using Cellquest software (BD Biosciences). Data were analyzed using Flowjo software (Treestar, Ashland, OR, USA).

2.12. Transmission Electron Microscopy (TEM)

Cells were pelleted and fixed in 2.5% glutaraldehyde (Electron Microscopy Sciences, U.S.A) diluted in 0.1 M sodium cacodylate buffer, pH 7.2 (Electron Microscopy Sciences) overnight. Cells were then rinsed with sodium cacodylate buffer twice, postfixed for 2 h in 2% osmium tetroxide at room temperature, washed with distilled water, and stained with 0.5% uranyl acetate at 4°C overnight. Samples were then dehydrated in successive ethanol washes, followed by infiltration of 1 (100% ethanol): 1 (Spurr's resin). Samples were kept overnight embedded in 100% Spurr's resin, mounted in molds and left to polymerize in an oven at 56°C for 48 h. Ultrathin sections (70–90 nm) were cut with an ultramicrotome, EM UC7 (Leica, Germany). Sections were stained with uranyl acetate and lead citrate and subsequently viewed using a JEM1010 transmission electron microscope (JEOL, Japan).

2.13. Measurement of intracellular ATP content

To quantify metabolically active cells, intracellular ATP levels were measured by CellTiter-Glo Luminscent Cell Viability Assay (Promega, Cosmogenetech, Seoul, South Korea) following the manufacturer's protocol.

2.14. Measurement of caspase 3/7 activity

Activation of caspase 3/7 was measured by using the Caspase-Glo 3/7 Assay (Promega, Madison, WI, USA) according to the manufacturer's instructions. Caspase 3/7 reagent was added with at 1:1 ratio to the sample volume, and the cells were incubated for 1 h at room temperature. The luminescence of each sample in triplicates was measured using a microplate reader.

2.15. Whole cell extracts and western blotting

For preparation of whole cell extracts, cells were harvested, washed in cold 1xPBS, and lysed in Mammalian Protein Extraction Reagent (M-PER™, ThermoFisher, Waltham, Massachussetts, USA) supplemented with 1 x protease inhibitor cocktail (Complete, EDTA-free, Roche, Basel, Switzerland) according to the manufacturer's instructions. Protein concentration was measured using the Bradford assay. Proteins were aliquoted and stored at -80°C. Afterwards, proteins were subjected to sodium dodecylsulfate (SDS)–polyacrylamide gel electrophoresis (PAGE) and transferred to PVDF membranes (GE Healthcare, Little Chalfont, UK). Blots were probed in PBS-T containing the appropriate blocking agent (5% milk or 5% BSA) for 1 hour. Membranes were pre-hybridized overnight with the indicated primary antibodies. After washing, blots were incubated with species-appropriate HRP-conjugated secondary antibody (Santa Cruz) in PBS-T containing 5% milk. Proteins of interest were detected with ECL Plus Western blotting Detection System reagent (GE Healthcare) using ImageQuant LAS 4000 mini system (GE Healthcare).

2.16. Statistical Analysis

Data are expressed as the mean ± SD and significance was estimated by using one-way or two-way ANOVA (analysis of variance) using Prism 8 software, GraphPad Software (La Jolla, CA, USA). P-values were considered statistically significant when $p < 0.05$. Legends are represented as follows: $*p < 0.05$, $**p < 0.01$, $***p < 0.001$.

3. RESULTS

3.1. Aplysinopsin Analogs Display Cytostatic and Cytotoxic Activities in Myeloid Leukemia Cells.

Aplysinopsin (EE-115) and its analogs EE-31, EE-80, EE-84, EE-92 and EE-118 (Figure 1) were tested for their anti-leukemic effects on myeloid leukemia cell lines K562 and U937 using the trypan blue exclusion test (Tables 1 and 2, Figure 2).

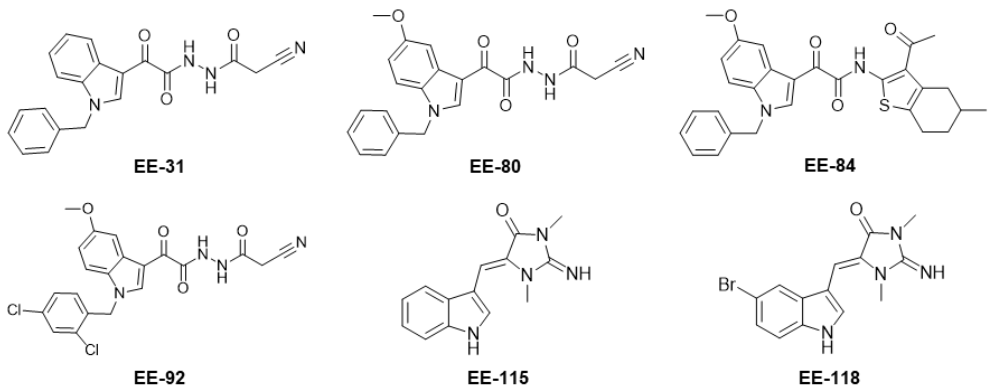

Figure 1. Chemical structures of aplysinopsin (EE-115) and its analogues (EE-31, EE-80, EE-84, EE-92, EE-115)

Table 1. GI_{50} of aplysinopsin analogues in myeloid leukemia cell lines. GI_{50} (μM) values were evaluated after indicated times of compound treatment

		GI_{50} (μM)		
Compound	**Cell Line**	**24h**	**48h**	**72h**
EE-31	K562	> 50	> 50	> 50
	U937	> 50	> 50	> 50
EE-80	K562	> 50	> 50	> 50
	U937	> 50	> 50	> 50
EE-84	K562	> 50	32.22 ± 3.91	19.07 ± 0.80
	U937	> 50	27.78 ± 1.48	21.51 ± 1.91
EE-92	K562	> 50	> 50	> 50
	U937	> 50	> 50	46.38 ± 4.04
EE-115	K562	> 50	> 50	> 50
	U937	> 50	> 50	> 50
EE-118	K562	7.59 ± 0.46	8.34 ± 0.31	8.25 ± 0.33
	U937	10.64 ± 0.39	8.75 ± 0.58	10.29 ± 0.31

Table 2. IC_{50} of aplysinopsin analogues in myeloid leukemia cell lines. IC_{50} (μM) values were evaluated after indicated times of compound treatment

		IC_{50} (μM)		
Compound	**Cell Line**	**24h**	**48h**	**72h**
EE-31	K562	> 50	> 50	> 50
	U937	> 50	> 50	> 50
EE-80	K562	> 50	> 50	> 50
	U937	> 50	> 50	> 50
EE-84	K562	> 50	> 50	> 50
	U937	> 50	> 50	> 50
EE-92	K562	> 50	> 50	> 50
	U937	> 50	> 50	> 50
EE-115	K562	> 50	> 50	> 50
	U937	> 50	> 50	> 50
EE-118	K562	17.51 ± 0.61	16.75 ± 0.36	16.50 ± 0.68
	U937	9.25 ± 0.18	8.71 ± 0.16	8.61 ± 0.27

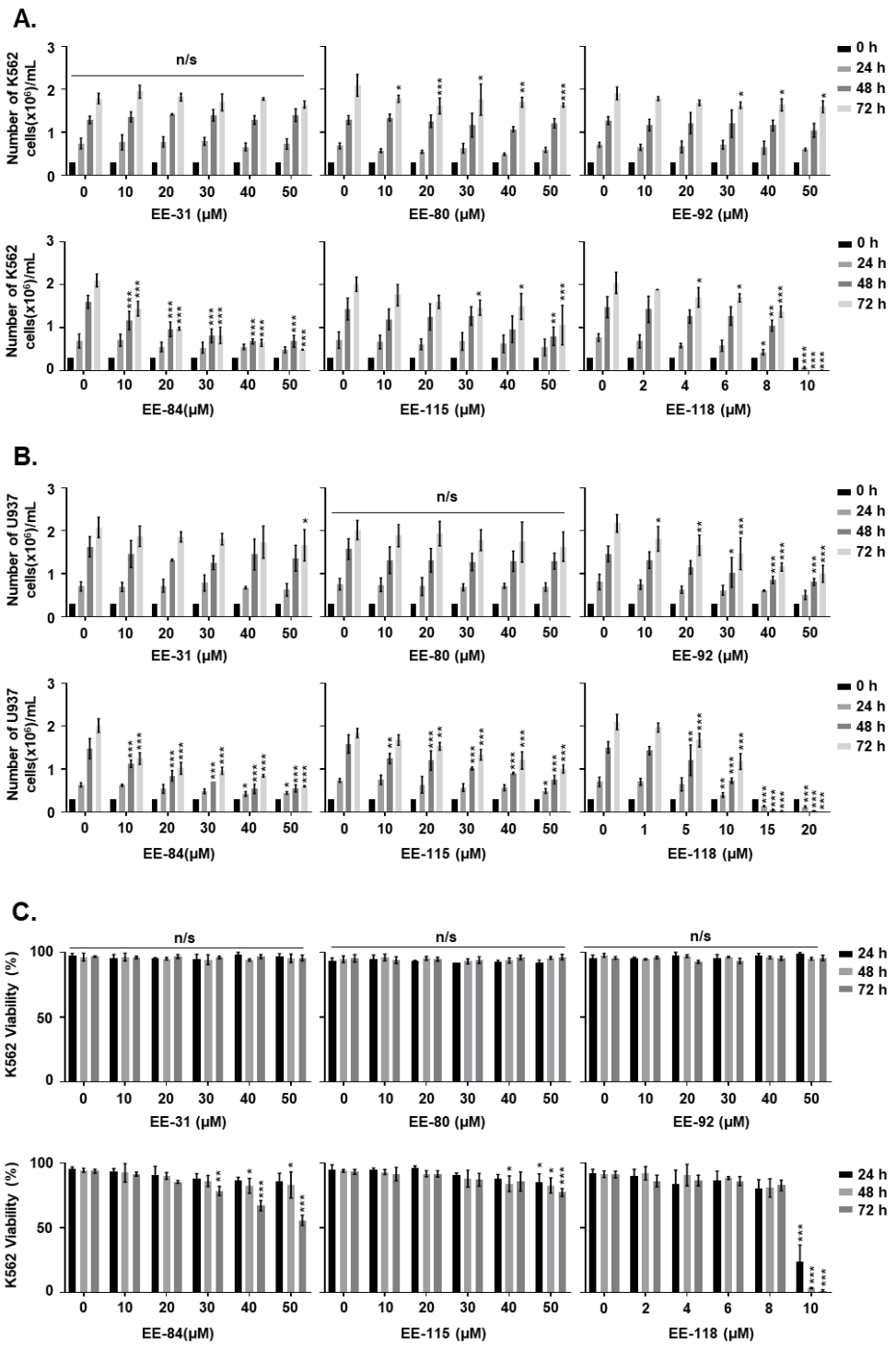
A.
Number of K562 cells(x10^6)/mL
n/s
0 h
24 h
48 h
72 h
EE-31 (μM)
EE-80 (μM)
EE-92 (μM)
EE-84(μM)
EE-115 (μM)
EE-118 (μM)
B.
Number of U937 cells(x10^6)/mL
C.
K562 Viability (%)
24 h
48 h
72 h

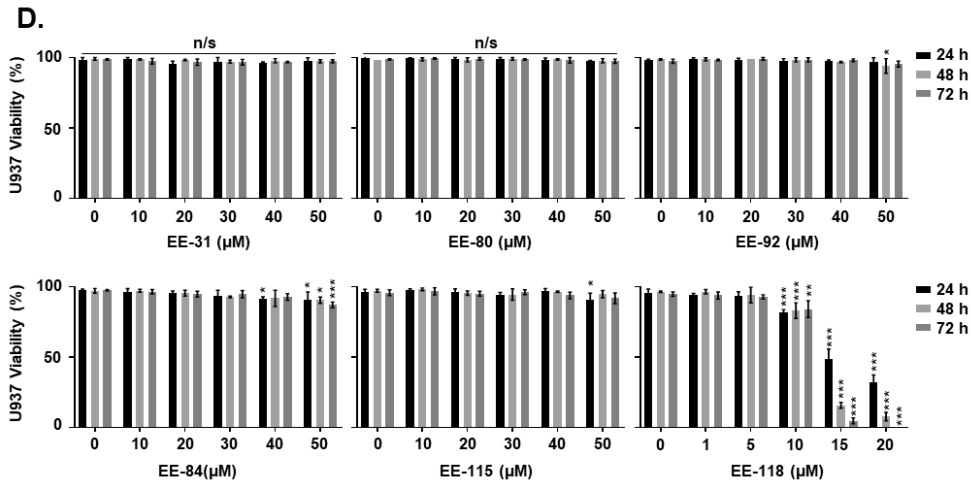

Figure 2. Effect on proliferation and viability of aplysinopsin-treated leukemia cells, U937 and K562 (A-D) After 24, 48, and 72 h of treatment on U937 and K562 cells, cell number (A-B) and viability (C-D) were determined by trypan blue exclusion test. All data are expressed as mean ± SD of three independent experiments; *p<0.05, **p<0.01, **p<0.001 compared with controls.

Treatment of K562 and U937 cells at various concentrations of aplysinopsins after 24, 48, and 72 hours showed cytostatic and cytotoxic activities. While EE-31, EE-80 and EE-115 neither affected the proliferation nor viability of K562 and U937 cells at concentrations up to 50 µM, derivatives EE-84, EE-92, and EE-118 displayed anti-proliferative effects in both cell lines in a dose- and time-dependent manner. After 72 hours, EE-84 and EE-118 significantly affected proliferation of K562 and U937 cells. (Table 1, Figure 2A-B). Interestingly, EE-118, a brominated analog of EE-115, induced cytotoxicity in both leukemic cell lines at concentrations 10 µM after 24 hours. EE-118 IC_{50} values reached 10.29 µM and 8.25 µM in U937 and K562 cells at 72 hours, respectively (Table 2, Figure 2C-D).

EE-84 and EE-118 were selected for further study. EE-115, the parental compound, was used as a control. I validated the differential cytostatic/cytotoxic profiles of aplysinopsin and its derivatives by colony formation assays (CFA), allowing the assessment of the compound's effects on the clonogenic potential of treated U937 and K562 cells in a 3D culture environment (Figure 3A-C). Even though EE-84 showed better potential in inhibiting cellular growth in suspension cultures than EE-115, in CFA, EE-84 only reduced the total surface area and average size of colonies after a 48 h pretreatment, while the number of colonies remained similar over the range of increasing concentrations (Figure 3A). EE-115 dose-dependently decreased the number, total surface area, and average size of colonies, showing a significant reduction at 50 µM in both cell lines (Figure 3B). EE-118, on the other hand, inhibited colony formation at much lower concentrations, with a marked decrease of all criteria at 10 µM for K562 and 20 µM for U937 (Figure 3C) in line with the viability assays (Table 2, Figure 2).

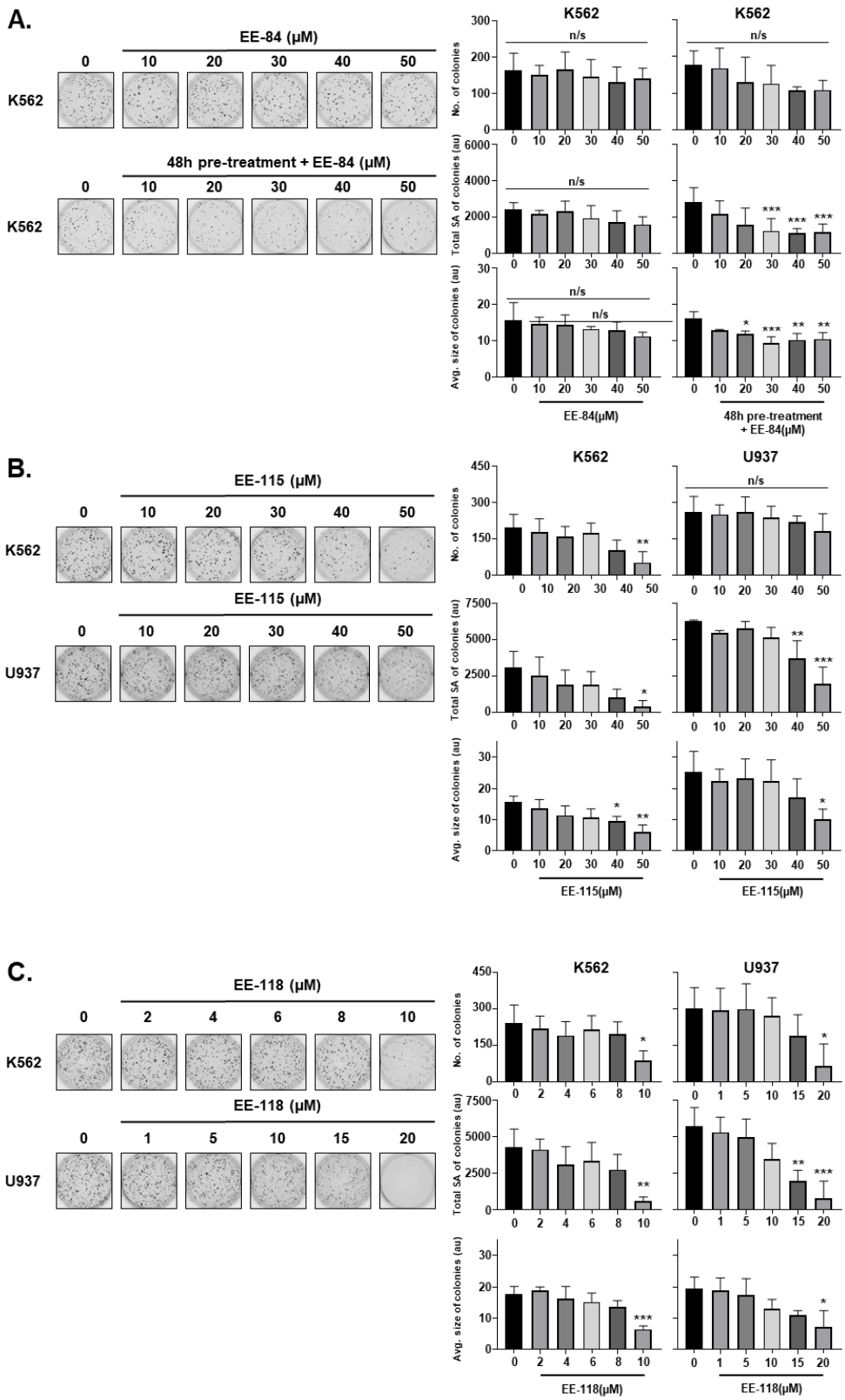
A.
EE-84 (μM)
0
10
20
30
40
50
K562
48h pre-treatment + EE-84 (μM)
K562
K562
No. of colonies
Total SA of colonies (au)
Avg. size of colonies (au)
n/s
EE-84(μM)
48h pre-treatment + EE-84(μM)
B.
EE-115 (μM)
K562
U937
U937
EE-115(μM)
C.
EE-118 (μM)
0
2
4
6
8
10
1
5
15
20
EE-118(μM)

Figure 3. Differential anti-leukemic effects observed by CFA after aplysinopsins treatments (A-C). Representative pictures of clonogenic assays after EE-84 treatment (A), EE-115 treatment (B), and EE-118 treatment (C) from three independent experiments are shown on the left. Corresponding quantifications (number of colonies, total surface area of colonies and average size of colonies) are indicated on the right. Statistical analysis was performed by one-way ANOVA, followed by Dunnett's multiple comparisons test. Differences were considered significant when $*p<0.05$, $**p<0.01$, $***p<0.001$ compared to control. n/s: not significant.

Considering the moderately cytotoxic effect of 50 μM EE-84 at 72 hours in K562 cells and the strong cytotoxicity of EE-118 at 24 hours in both U937 and K562 cells (Figure 2), I then investigated the cell death modalities induced by aplysinopsin derivatives using Hoechst/PI staining (Figure 4A-B). EE-84 reduced K562 cell viability at all concentrations resulting in about 11% of necrotic cells at 50 μM (Figure 4A). On the other hand, EE-118 displayed strong cytotoxicity starting at 10 μM and 15 μM in both K562 and U937 cells, respectively, by early and late apoptosis as well as necrosis (Figure 4B). In particular, EE-118 showed around 25%, 29%, and 12% of early apoptotic, late apoptotic, and necrotic cell death in K562 cells, respectively. Bcr-Abl inhibitor imatinib (1 μM) and topoisomerase inhibitor etoposide (100 μM) were used as bona fide controls for K562 and U937 cells. Altogether, I show that aplysinopsin (EE-115) and its derivatives (EE-84 and EE-118) exhibit anti-leukemic activities, certifying further investigations of these compounds.

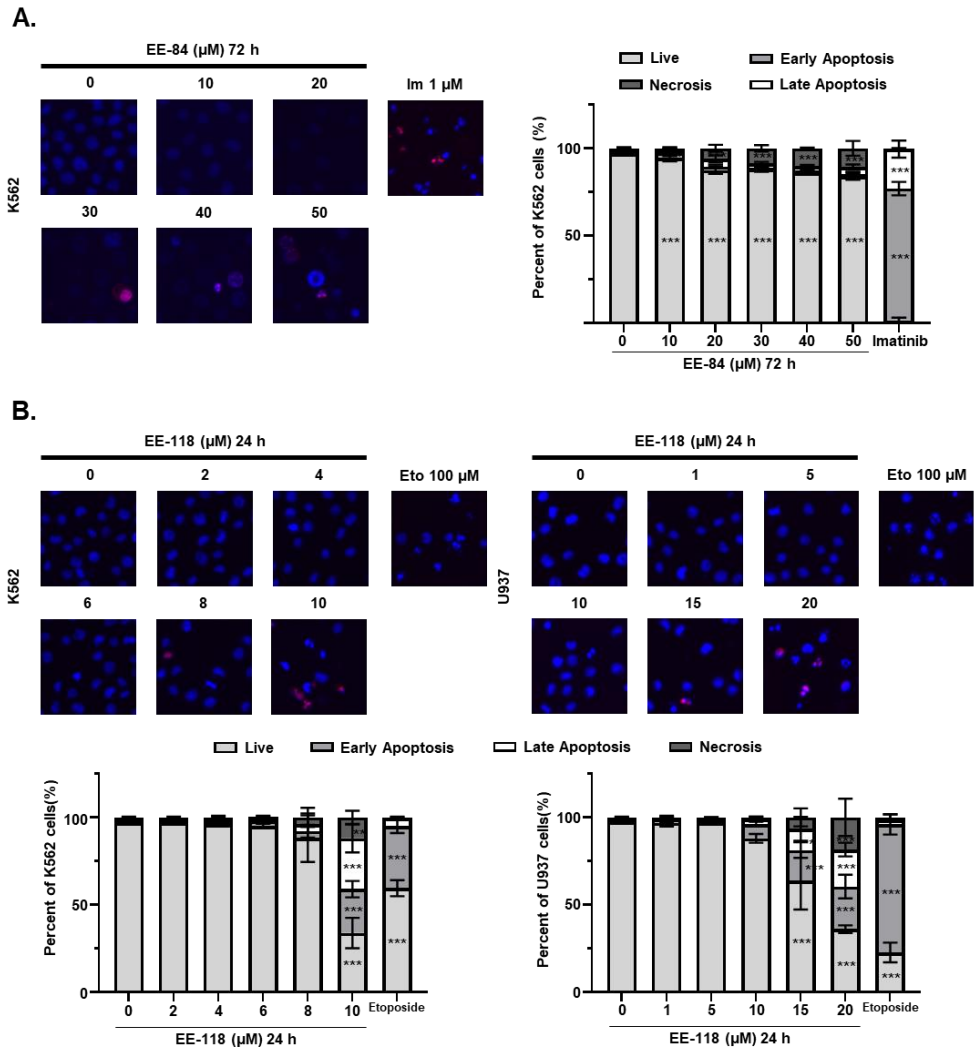

Figure 4. Percentage of different cell death modalities after increasing concentrations of EE-84 treatment in K562 (A) and EE-118 treatment in K562 and U937 cells (B). Representative microscopy images of Hoechst 33342/PI double-stained nuclei of K562 and U937 cells exposed to different concentrations of aplysinopsin derivatives at indicated times are shown. Apoptotic or necrotic cells were calculated from three independent experiments. Im: imatinib (1 μM); Eto: etoposide (100 μM). All data are expressed as mean ± SD of three independent experiments. Statistical analysis was performed by two-way ANOVA, followed by Dunnett's multiple comparisons test; *p<0.05, **p<0.01, ***p<0.001 compared to controls.

3.2. Drug Likeness of Compounds EE-84, EE-115, and EE-118

After assessing the anti-cancer effects of aplysinopsin and its derivatives on leukemic cell lines, I examined the drug-likeness of the three aplysinopsins (EE-84, EE-115, and EE-118) according to Lipinski's rule of five, which describes the druggability of a particular chemical molecule (Table 3) [11]. A molecule is orally active when there are no more than 5 H bond donors, no more than 10 H bond acceptors, the molecular mass is less than 500 Daltons, and the octanol-water partition coefficient LogP is not greater than 5. EE-115 and EE-118 do not violate any of the above-mentioned conditions.

Table 3. *In silico* prediction for the drug likeliness of EE-84, EE-115, and EE-118. Drug likeliness of the aplysinopsin derivatives were calculated and interpreted based on Lipinski's rule of five.

	EE-84	**EE-115**	**EE-118**
Mass	500.00	254.00	319.00
Hydrogen bond donor	1	2	0
Hydrogen bond acceptor	5	4	3
LogP	5.91	1.85	1.12
Molar reactivity	142.51	74.54	65.88

3.3. Safety Profiles of EE-84, EE-115, and EE-118 based on RPMI1788 / K562 Differential Toxicity and Zebrafish Toxicity Assays

To assess the cytotoxicity of EE-84, EE-115, and EE-118 on healthy models *in vitro* and *in vivo*, and to confirm the aplysinopsins' safety profile, I first treated a non-cancerous cell line RPMI1788 with different concentrations of aplysinopsins EE-84, EE-115, and EE-118 (Table 4-5, Figure 5). EE-115 and EE-118 induced a greater anti-proliferative effect in RPMI1788 cells than in leukemic cell lines K562 and U937. The GI_{50} of EE-115 and EE-118 for the RPMI1788 cell line were lower than those for the leukemia cell lines (Figure 2, 5, Table 1 ,4). EE-84, however, showed a differential effect in the non-cancerous cell line as the GI_{50} for RPMI1788 were at all time-points higher compared to that for K562 cells (Figure 6, Table 1, 4), highlighting K562 cells' sensitivity to EE-84 in comparison to RPMI1788 cells.

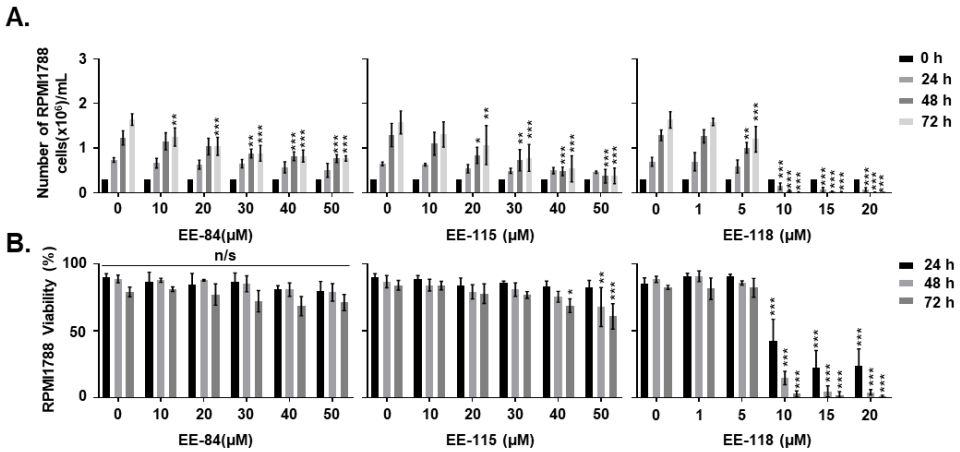

Figure 5. Effect on the proliferation and viability of EE-84, EE-115 and EE-118 on non-cancerous cell line RPMI1788. (A) Proliferation and (B) viability of aplysinopsin-treated RPMI1788 were assessed by trypan blue exclusion test. All data are expressed as mean ± SD of three independent experiments; *p<0.05, **p<0.01, ***p<0.001 compared with controls.

Table 4. GI_{50} of aplysinopsin analogs in RPMI1788 cell line. GI_{50} (μM) values were evaluated after indicated times of compound treatment

	GI_{50} (μM)		
Compound	**24h**	**48h**	**72h**
EE-84	> 50	> 50	40.10 ± 3.79
EE-115	> 50	30.36 ± 1.95	27.72 ± 2.30
EE-118	7.43 ± 0.47	6.07 ± 0.11	5.66 ± 0.93

Table 5. IC_{50} of aplysinopsin analogs in RPMI1788 cell line. $IC1_{50}$ (μM) values were evaluated after indicated times of compound treatment

	IC_{50} (μM)		
Compound	**24h**	**48h**	**72h**
EE-84	> 50	> 50	> 50
EE-115	> 50	> 50	> 50
EE-118	11.04 ± 0.90	7.91 ± 0.28	7.55 ± 0.91

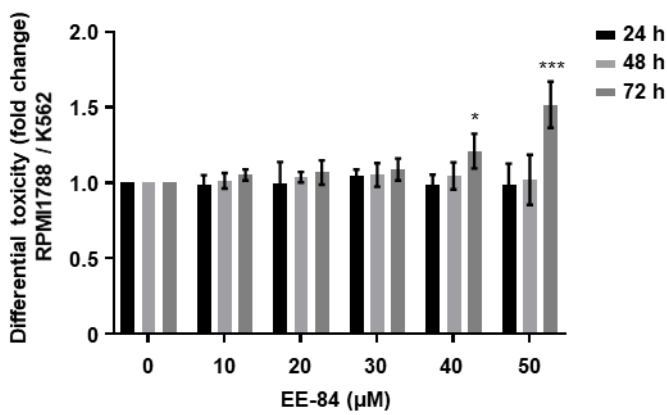

Figure 6. Differential toxicity of EE-84 in RPMI1788 and K562 cells. Differential toxicity (RPMI788/K562) of EE-84 was determined by trypan blue exclusion test; Data represents the mean ± SD of three independent experiments. Statistical analysis: two-way ANOVA with Dunnett's multiple comparison test; *p<0.05, **p<0.01, ***p<0.001 compared to controls.

Zebrafish embryos were also treated 24 h post-fertilization (hpf) to validate the *in vivo* safety profiles of the aplysinopsin compounds. The zebrafish were observed after 24 h of exposure to different aplysinopsin concentrations (Figure 7A-D). Concentrations up to 50 µM of EE-118 and up to 100 µM of EE-84 and EE-115 did not affect the survival rate of zebrafish (Figure 7B), and there were no significant morphological changes observed at the different concentrations of the compounds (Figure 7C). EE-115 and EE-118 did not trigger cardiotoxicity as the heart rate stayed within the range of the control zebrafish group (Figure 7D). Altogether, I considered EE-84 as a safe compound considering the differential effect *in cellulo* (Figure 7). EE-84 did not affect viability of zebrafish embryos even at the highest concentration of 100 µM despite the decreased heart rate. Based on these results we decided to investigate the molecular and cellular effects of this compound.

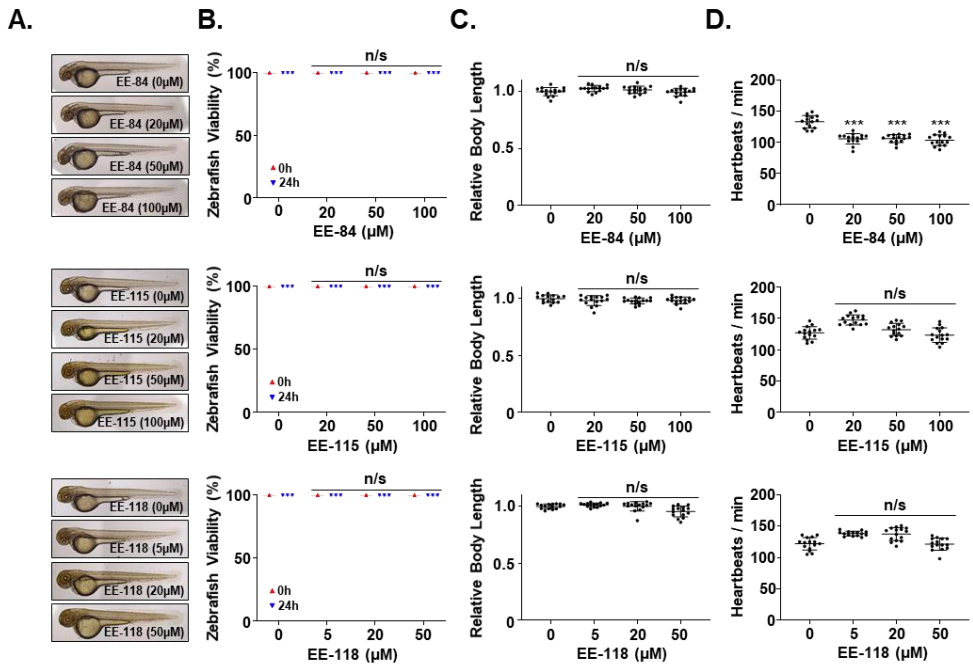

Figure 7. Effect of aplysinopsin derivatives on zebrafish. Zebrafish toxicity assays were performed by treatment of aplysinopsin compounds at indicated concentrations. (A) Representative pictures of zebrafish are shown. Zebrafish viability (B), relative body length (C) and heartbeats/min (D) were measured. Data represents a total of fifteen fish per group. Ordinary one-way ANOVA followed by Dunnett's post hoc test revealed significant differences indicated by ***p<0.001 compared to control. n/s: not significant.

3.4. EE-84 Induces Cell Cycle Dysregulation

To better understand the possible mechanism of EE-84-induced cell growth inhibition in K562 cells, cell cycle progression was investigated by flow cytometry (Figure 8). I observed a significant decrease of 7.0% and 7.5% in the G2/M cell population at 30 and 50 µM EE-84 treatment after 48 hours respectively. After 72 h of EE-84 treatment at 30 and 50 µM, 7.2% and 10.3% of cell population was decreased in the G1 phase compared to DMSO-treated control, respectively. Similarly, increased levels of cells in the S phase were observed compared to controls. I also validated that the concentrations of EE-84 used are cytostatic as the sub-G_1 population for all concentrations remained under 12%. Celecoxib (40 µM), known to arrest cells in the G1 phase, was used as *bona fide* control.

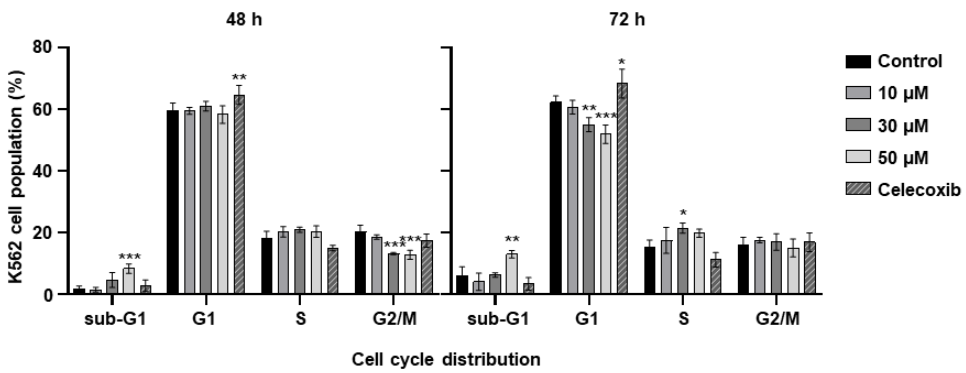

Figure 8. EE-84 induced cell cycle dysregulation after 48 and 72 h in K562 cells. For cell cycle analysis, K562 cells were treated with 10, 30, and 50 µM EE-84 for 48 and 72 h. Cells were then harvested and fixed with 70% ethanol for at least one hour. Cells were stained with propidium iodide for 30 min at 37°C. Cell distribution of each phase of cell cycle was determined by flow cytometric analysis. Data represents the mean ± SD of three independent experiments. Two-way ANOVA with Dunnett's post comparisons tests: *p<0.05, **p<0.01, ***p<0.001 compared to controls.

3.5. EE-84 Induces Morphological Changes in the CML cell line, K562

As the next step, the morphology of EE-84 treated K562 cells was examined. At 50 μM of EE-84, aberrant increase in the cell size over the time was seen (Figure 9A). The appearance of vacuoles increased time-dependently up to 96 hours. To better analyze the morphological changes induced by increasing EE-84 dose and time exposure, I assessed cell size and granularity by flow cytometry (Figure 9B). Compared to DMSO-treated controls, EE-84-treated K562 cells showed a progressive increase in the values of forward scatter (a.u.) and side scatter (a.u.) as measurements of cell size and granularity, respectively.

Morphological changes were examined in detail by transmission electron microscopy (Figure 9C). K562 cells treated by EE-84 at 30 μM underwent mitochondrial damage after 24 h, 48 h, and 72 h of compound exposure as well as mitophagy. In contrast, there were no abnormal morphological changes in DMSO-treated control negative K562 cells.

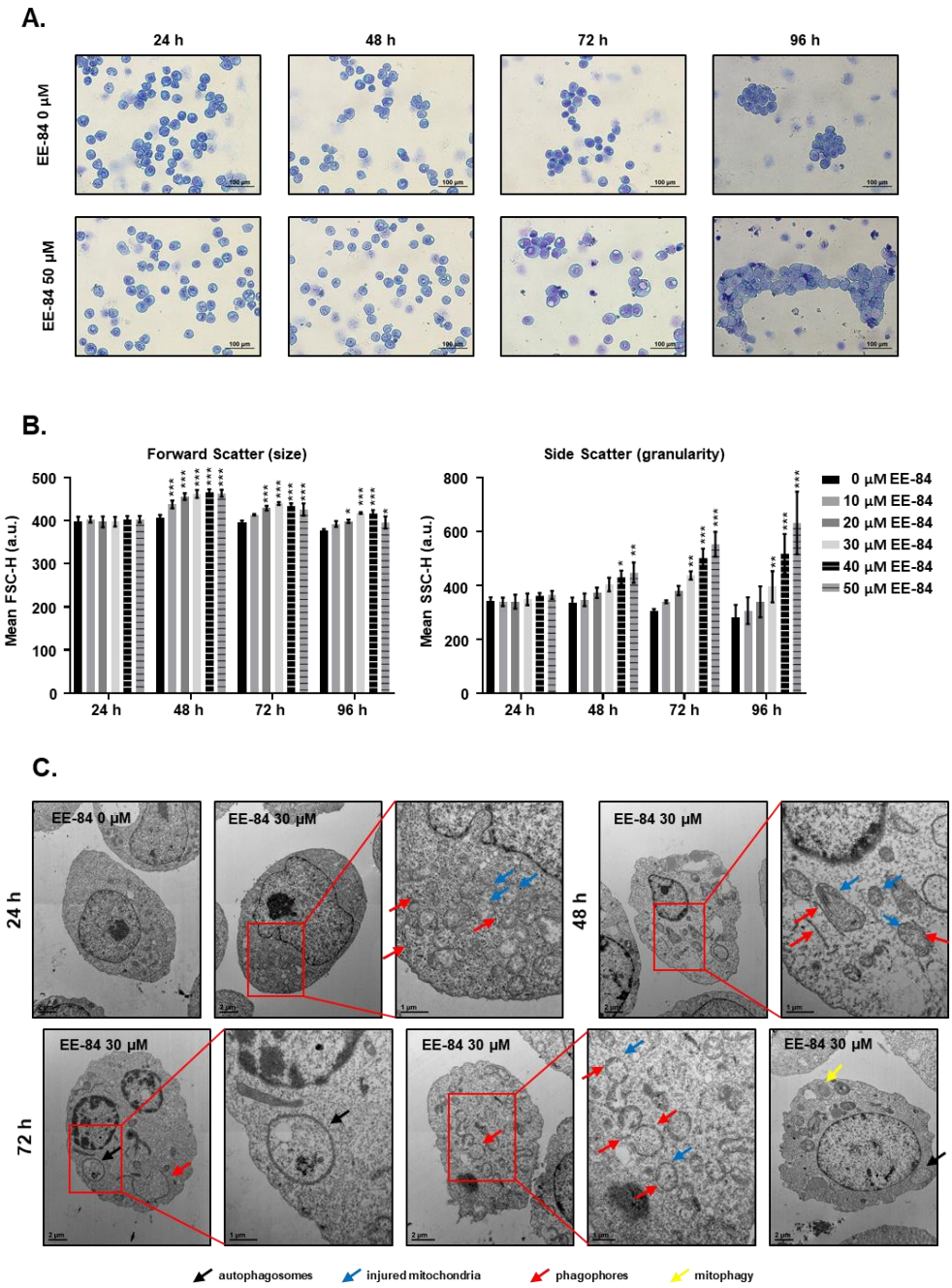
A.
24 h
48 h
72 h
96 h
EE-84 0 µM
EE-84 50 µM
B.
Forward Scatter (size)
Side Scatter (granularity)
Mean FSC-H (a.u.)
Mean SSC-H (a.u.)
0 µM EE-84
10 µM EE-84
20 µM EE-84
30 µM EE-84
40 µM EE-84
50 µM EE-84
C.
EE-84 0 µM
EE-84 30 µM
EE-84 30 µM
EE-84 30 µM
EE-84 30 µM
EE-84 30 µM
24 h
48 h
72 h
autophagosomes
injured mitochondria
phagophores
mitophagy

Figure 9. Morphological changes of K562 cells treated with EE-84. (A) K562 cells were treated with 50 μM EE-84 for 24, 48, 72 and 96 hours. Light microscopy at magnification 200x was used for morphological observation. (B) K562 cells were treated with indicated concentrations of EE-84 for up to 96 hours. At the time points of interest, cells were harvested and analyzed by flow cytometry using forward (relative cell sizes) and side scatter (granularity) measurements. For morphological analysis of EE-84 exposed K562 cells debris was excluded. Results are the mean ± SD of three independent experiments. Statistical analysis was performed by two-way ANOVA, followed by Dunnett's multiple comparisons test; $*p<0.05$, $**p<0.01$, $***p<0.001$ compared to controls. (C) Transmission electron microscopy at magnifications of 8,000x or 10,000x (whole cells) and 20,000x or 25,000x (cell details). Cells were treated with 30 μM EE-84 and were exposed for up to 72 hours. Phagophores, autophagosomes, and injured mitochondria, and incidence of mitophagy are highlighted by red, black, blue and yellow arrows, respectively. DMSO-treated K562 cells at 24 hours were used as a control.

3.6. EE-84 Sensitizes K562 Cells Against Mcl-1 Inhibitor A-1210477 and Shows Synergistic Cytotoxicity in K562 cells

Considering the cytostatic potential but limited cytotoxicity of EE-84, I then investigated the expression levels of the anti-apoptotic protein, Mcl-1, which may be responsible for the apoptotic blockage. Based on the increase of anti-apoptotic Mcl-1 expression in EE-84-treated K562 cells after 24, 48, and 72 h compared to control expressed in fold change (Figure 10), speculated that the combined treatment of the specific Mcl-1 inhibitor A-1210477 with EE-84 may sensitize K562 cells to apoptotic cell death. Using subtoxic concentrations of EE-84 (20 µM and 30 µM) and A-1210477 (10 µM), I first assessed the combinatory effects of these compounds using Hoechst/PI staining after 24 hours (Figure 11A). 44% and 53% increase of apoptotic cell death in combinatory treatments compared to DMSO-treated control was observed, respectively. To identify whether the combination treatments are synergistic, the combination index (CI) of each compound-pair was calculated (Figure 11B, Table 5). The obtained values for the two compound combinations denoted synergism, and 30 µM of EE-84 with 10 µM of A-1201477 were selected for further studies.

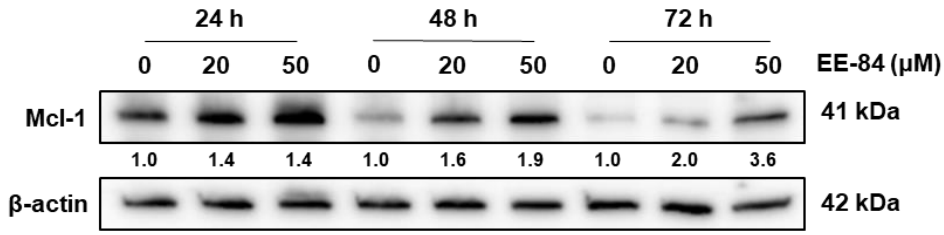

Figure 10. EE-84 increased expression levels of anti-apoptotic protein Mcl-1 compared to DMSO-treated control. K562 cells were treated with varying concentrations of EE-84 for 24, 48, and 72 hours. The effects on Mcl-1 and β-actin were determined by Western blot analysis. Western blot data are interpreted in terms of fold changes in protein expression compared to control at the corresponding time point. The values represent the average of 3 independent experiments.

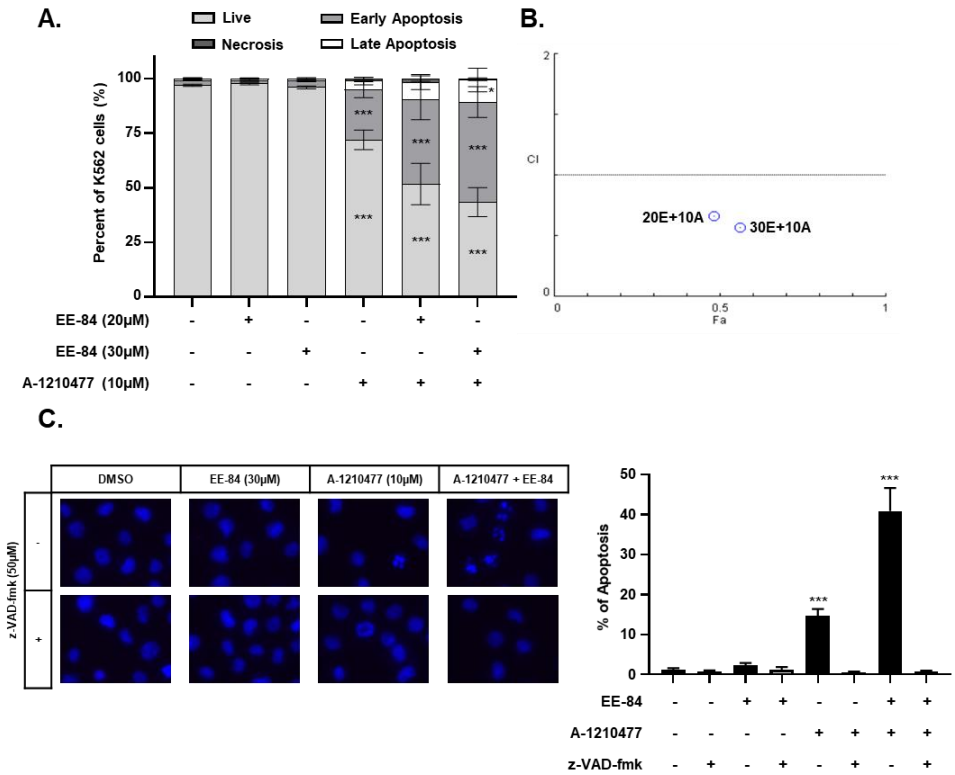

Figure 11. EE-84 sensitizes CML cells to BH3 mimetics. (A) 24 h co-treatment analysis of 20 μM and 30 μM EE-84 with 10 μM A-1210477 using Hoechst 33258/PI staining showed an increase in apoptotic cell death compared to single treatments of compounds. (B) The plot representing the fraction affected-combination index (Fa-CI) of the treatment of K562 cells with EE-84 and A-1210477 after 24 h was obtained with Compusyn software. (C) Selection of the optimal compound combination of 30 μM EE-84 and 10 μM A-1210477 is analyzed by Hoechst/PI staining. z-VAD-fmk was used as a pan-caspase inhibitor. Data are expressed as mean ± SD of three independent experiments. Statistical analysis was performed by one-way or two-way ANOVA, followed by Dunnett's multiple comparisons test; *p<0.05, **p<0.01, ***p<0.001 compared to controls.

Table 5. Combination values of EE-84 and A-1201477 treatment obtained by Compusyn software

EE-84 (μM)	A-1210477 (μM)	Fa	CI
20	10	0.483	0.66
30	10	0.563	0.57

To evaluate whether the induction of apoptosis by combination treatment is caspase-dependent, I treated K562 cells with a broad-spectrum caspase inhibitor z-VAD-fmk together with single and combined treatments of EE-84 and A-1210477, and evaluated the percentage of apoptotic cells *via* Hoechst/PI staining (Figure 11C). A-1210477 and the combined treatment induced 14.67 ± 1.73% and 40.89 ± 5.75% of apoptotic cell death, respectively. The addition of z-VAD-fmk completely abrogated the cytotoxic effects.

The cytotoxic effect was also validated through the quantification of intracellular ATP levels. ATP levels decreased significantly for the combination treatment compared to the compound treatments alone (Figure 12A). 1 h pre-treatment of z-VAD-fmk showed an increase in cell viability with the single treatment of 10 μM A-1210477. This was also observed with the combined treatment. The addition of the caspase inhibitor showed no significant difference in the ATP levels for the single treatment of 30 μM EE-84. To further validate our data, the activity of caspase-3/7 levels were measured. The significant 5.52-fold increase of caspase 3/7 activity obtained after the combined treatment of EE-84 and the Mcl-1 inhibitor in comparison to the untreated control reaffirms the synergistic effect of the two compounds (Figure 12B). To examine the detailed mechanism by which the combined treatment acts, I studied the intrinsic and extrinsic apoptotic pathways in K562 cells by Western Blot (Figure 12C-E). First, the expression level of caspase 8, a cysteine protease that initiates apoptotic signaling *via* the extrinsic pathway, was detected. Cleavage of pro-caspase 8 in the combined treatment was observed (Figure 12C). Our results showed a reduction of pro-caspase-9, the initiator caspase critical for the intrinsic pathway, concomitant with the appearance of a cleaved fragment at 18 kDa after the combined treatment. In line with the previous observation of increased caspase-3/7 activity for the combination treatment, I observed a strong

cleavage of pro-caspase 3 as well as cleaved fragments of caspase 7 for the combined treatment (Figure 12D). Our evaluation of anti-apoptotic Mcl-1 expression levels showed an increase of Mcl-1 in EE-84 (30 μM) and A-1210477 (10 μM) single treatments as well as in the combined treatment in line with the stabilization/inactivation of these proteins as suggested by previous studies (Figure 12E) [12, 13].

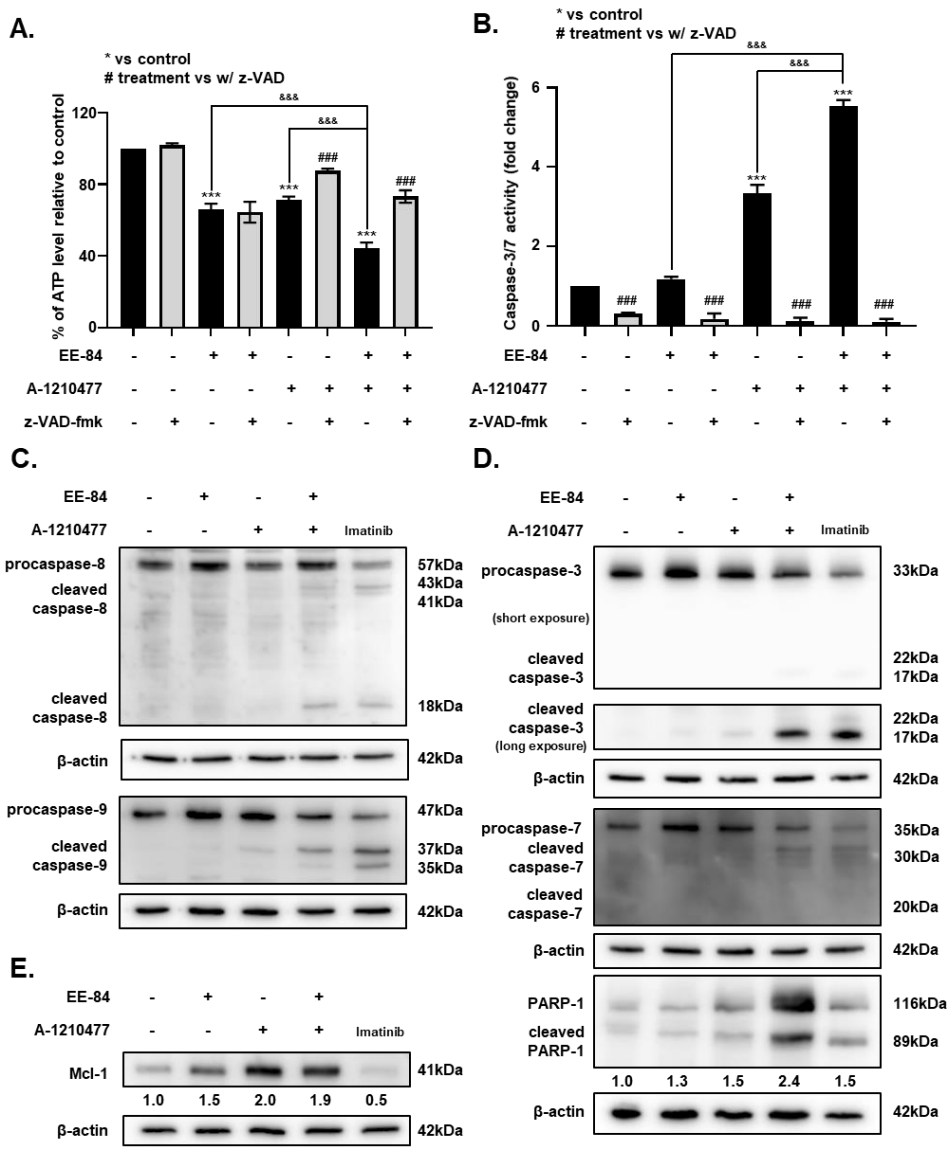

Figure 12. Caspase-dependent induction of apoptosis in K562 cells by EE-84 in synergism with the Mcl-1 inhibitor A-1210477. (A) K562 cell viability was determined by the measurement of cellular ATP content using the CellTiter-Glo assay. K562 cells were pre-treated at the concentration of 50 μM z-VAD-fmk for 1 h before exposure to the compounds. (B) Effects of single or combination treatments of EE-84 and A-1210477 with or without z-vad FMK on caspase-3/7 activity in K562 cells. Three separate experiments were performed for both CellTiter-Glo and caspase 3/7 assays, and each condition was measured in three replicate wells. Values are the mean ± SD of three independent experiments. The asterisk indicates value

significantly different from the control; *p<0.05, **p<0.01, ***p<0.001. (C-E) Western blots showing expression levels of apoptosis-related proteins after single or combination treatments of EE-84 and A-1210477 in K562 cells. (C) Results of expression levels of initiator caspases, caspase 8 and 9; (D) expression levels of effector caspases, caspase 3 and 7, and PARP-1; (E) and expression levels of anti-apoptotic protein Mcl-1 are displayed. Protein expression levels of cleaved PARP-1 and Mcl-1 are quantified and expressed in fold changes relative to control. The values represent the average of 3 independent experiments.

4. DISCUSSION

The marine ecosystem represents a huge and largely untouched reservoir of bioactive secondary metabolites from various marine organisms. The variety of environmental conditions such as water pressure, temperature, light, salt contents etc. oblige marine life to adapt and as a result their biochemical machinery has developed to wrestle such varying environmental pressures [14]. Possessing unique structural motifs and pharmacological activities, the resulting natural products from these marine flora and fauna have provided a wealth of lead molecules with medicinal value and has played a leading role in drug discovery research. In fact, there have been numerous scientific findings identifying natural products of marine origins as modulators of cell death, exerting cytotoxic effects on cancer cells as activators of apoptosis, autophagy or oncosis [15]. However, thousands if not millions of marine-derived compounds with anti-cancer potential are yet to be uncovered. Further pharmacological investigations of marine-derived products and their analogs may therefore provide new insights into the discovery of novel chemotherapeutic drugs [16].

Currently, seven marine-based drugs have been approved for marketing, 23 compounds are in clinical trials between phases I and III and thousands of compounds have been isolated from marine life and are undergoing preclinical studies [17]. Among those, four are used for cancer treatment: cytarabine (Cytosar®), trabectedin (Yondelis®), eribulin mesylate (Halaven®) and the conjugated antibody brentuximab vedotin (Acentris®) [18]. Cytosine arabinoside (cytarabine), which was originally isolated from the sponge *Cryptothethya crypa*, and now produced synthetically, shows particular success in the pharmaceutical market as one of the most effective drugs for the treatment of acute myeloid leukemia [19, 20]. In addition, trabectedin, a marine metabolite of *Ecteinascidia turbinata,* is used for the treatment of soft tissue sarcoma [21]. Despite the broad array of marine compounds already out in the market, as well as in the drug pipeline, there is still an enormous library of natural products that is untapped.

Aplysinopsins, which are a class of marine indole alkaloids, comprise two main distinct moieties – an indole and an imidazolidinone ring – and are a class of tryptophan-derived indole alkaloids that are isolated from a variety of marine

organisms, including sponges [22], corals [23], anemone [24], and mollusks [25-27]. Aplysinopsins, which was first isolated by Kazlauskas *et al*, was initially identified as the major metabolite of eight Indo-Pacific sponge species of the genera *Thorecta* [10]. Since then, there have been many discoveries of aplysinopsin derivatives from sponges namely: *Verongia spengeli*, *Dercitus* sp., *Smenospongia aurea*, *Verongular rigida*, *Dictyoceratida* sp., *Aplysinopsis reticulata*, *Aplysina* sp., *Hyrtios erecta*, and *Thorectandra* [25]. In line with the effort to identify new aplysinopsins with therapeutic potential, I report here a set of synthetic aplysinopsin derivatives that possess anti-leukemic effects against AML and CML cell lines. The derivatives displayed a range of cytostatic and cytotoxic effects, some affecting U937 and K562 cells more than others.

Moreover, I investigated the safety profiles of aplysinopsin derivatives *in vitro* and *in vivo* by treatment against healthy models such as RPMI1788 cells and zebrafish. This study acts as an essential tool in identifying lead candidates from a library of compounds since characterization of compound safety as well as toxicity patterns are of utmost importance for a successful drug development process. It can also be considered useful in predicting clinical adverse effects in the future [28]. Through this process, I discarded EE-118, a more cytotoxic agent against the non-cancerous cell line RPMI1788 in comparison to the myelogenous cell lines U937 and K562, and selected EE-84 for further studies.

The cytostatic nature of EE-84 was confirmed by cell cycle analysis; EE-84-treated K562 cells accumulated in the S phase concomitant with a decrease in the G1 phase at 72 hours. I also assessed the morphological changes that occurred in parallel to the cytostatic effect and identified an increase in cellular stress after 72 hours of treatment compared to control, confirmed by transmission electron microscopy. Other groups have identified cytostatic constituents of marine origins against cancer cell lines as well. For example, steroids derived from *Gymnacella dankaliensis* exhibited potent growth inhibition against a panel of 39 human cancer cell lines [29] and compounds isolated from Red Sea soft coral *Litophyton arboreum* demonstrated potent cytotoxic and/or cytostatic activity against HeLa and U937 cell lines [30]. Additionally, ecteinascidin-743 (ET-743), derived from the marine tunicate *Ecteinascidia turbinate*, showed an induction of apoptotic response in human cancer

cells and the accumulation of cells in S phase and a G2/M arrest when used at very low doses [31].

Evasion of apoptotic cell death by cancer cells can impair responses to anti-cancer therapy. Pro-survival B-cell lymphoma 2 (BCL-2) proteins play a role of perpetrators in this scenario, because they prevent apoptosis by keeping the cell death effectors like BAX and BAK under control [32]. BH3 mimetics offer a solution to this as they are designed to inhibit anti-apoptotic BCL2 family proteins, leading to BAX and BAK activation, and thus promoting apoptosis [33]. In particular, Mcl-1 has become a popular therapeutic target because it is one of the most frequently amplified genes across all human cancers and an increase in Mcl-1 expression is commonly associated with chemotherapy resistance [34]. In this study I evaluated the synergistic effect of EE-84, a cytostatic marine compound, with the Mcl-1 inhibitor A-1210477 against CML K562 cells. I showed that the co-treatment of the marine compound and the Mcl-1 inhibitor induced apoptotic cell death along with the activation of caspase activity. These results are in line with other studies in which BH3 mimetics like ABT199 showed synergism with cell stress inducers like cardiac glycosides [35] and coumarin derivatives [36].

In conclusion, I highlight the use of aplysinopsins as anti-leukemic agents. Our results identify compound EE-84 as a desirable drug candidate as it showed drug-like properties as well as safe profiling against healthy models *in vitro* and *in vivo*. The combination study of EE-84 with the BH3 mimetic A-1210477 treatment on K562 cells outlines the co-treatment as a potential therapeutic approach as it exponentially increased cell death otherwise not observed in the single treatment of EE-84.

5. REFERENCES

1. Dohner, H.; Weisdorf, D. J.; Bloomfield, C. D. Acute Myeloid Leukemia. *N. Engl. J. Med.* **2015,** *373*, 1136-52.
2. DiNardo, C. D.; Garcia-Manero, G.; Pierce, S.; Nazha, A.; Bueso-Ramos, C.; Jabbour, E.; Ravandi, F.; Cortes, J.; Kantarjian, H. Interactions and relevance of blast percentage and treatment strategy among younger and older patients with acute myeloid leukemia (AML) and myelodysplastic syndrome (MDS). *Am. J. Hematol.* **2016,** *91*, 227-232.
3. Zhao, J.; Song, Y.; Liu, D. Gilteritinib: a novel FLT3 inhibitor for acute myeloid leukemia. *Biomark. Res.* **2019,** *7*, 19.
4. Kang, Z. J.; Liu, Y. F.; Xu, L. Z.; Long, Z. J.; Huang, D.; Yang, Y.; Liu, B.; Feng, J. X.; Pan, Y. J.; Yan, J. S.; Liu, Q. The Philadelphia chromosome in leukemogenesis. *Chin. J. Cancer* **2016,** *35*, 48.
5. Iqbal, N.; Iqbal, N. Imatinib: a breakthrough of targeted therapy in cancer. *Chemother. Res. Pract.* **2014,** *2014*, 357027.
6. Bhamidipati, P. K.; Kantarjian, H.; Cortes, J.; Cornelison, A. M.; Jabbour, E. Management of imatinib-resistant patients with chronic myeloid leukemia. *Ther. Adv. Hematol.* **2013,** *4*, 103-117.
7. Molina, P.; Almendros, P.; Fresneda, P. M. Iminophosphorane-mediated imidazole ring formation: A new and general entry to aplysinopsin-type alkaloids of marine origin. *Tetrahedron* **1994,** *50*, 2241-2254.
8. Segraves, N. L.; Crews, P. Investigation of brominated tryptophan alkaloids from two thorectidae sponges: Thorectandra and Smenospongia. *J. Nat. Prod.* **2005,** *68*, 1484-8.
9. Newman, D. J.; Cragg, G. M. Natural Products as Sources of New Drugs from 1981 to 2014. *J. Nat. Prod.* **2016,** *79*, 629-61.
10. Kazlauskas, R.; Murphy, P. T.; Quinn, R. J.; Wells, R. J. Aplysinopsin, a new tryptophan derivative from a sponge. *Tetrahedron Lett.* **1977,** *18*, 61-64.
11. Lipinski, C. A.; Lombardo, F.; Dominy, B. W.; Feeney, P. J. Experimental and computational approaches to estimate solubility and permeability in drug discovery and development settings. *Adv. Drug. Deliv. Rev.* **2001,** *46*,

3-26.

12. Luedtke, D. A.; Niu, X.; Pan, Y.; Zhao, J.; Liu, S.; Edwards, H.; Chen, K.; Lin, H.; Taub, J. W.; Ge, Y. Inhibition of Mcl-1 enhances cell death induced by the Bcl-2-selective inhibitor ABT-199 in acute myeloid leukemia cells. *Signal Transduct. Target. Ther.* **2017,** *2*, 17012.
13. Tron, A. E.; Belmonte, M. A.; Adam, A.; Aquila, B. M.; Boise, L. H.; Chiarparin, E.; Cidado, J.; Embrey, K. J.; Gangl, E.; Gibbons, F. D.; Gregory, G. P.; Hargreaves, D.; Hendricks, J. A.; Johannes, J. W.; Johnstone, R. W.; Kazmirski, S. L.; Kettle, J. G.; Lamb, M. L.; Matulis, S. M.; Nooka, A. K.; Packer, M. J.; Peng, B.; Rawlins, P. B.; Robbins, D. W.; Schuller, A. G.; Su, N.; Yang, W.; Ye, Q.; Zheng, X.; Secrist, J. P.; Clark, E. A.; Wilson, D. M.; Fawell, S. E.; Hird, A. W. Discovery of Mcl-1-specific inhibitor AZD5991 and preclinical activity in multiple myeloma and acute myeloid leukemia. *Nat. Commun.* **2018,** *9*, 5341.
14. Lindequist, U. Marine-Derived Pharmaceuticals - Challenges and Opportunities. *Biomol. Ther.* **2016,** *24*, 561-571.
15. Folmer, F.; Jaspars, M.; Dicato, M.; Diederich, M. Marine cytotoxins: callers for the various dances of death. *Gastroenterol. Hepatol. Bed Bench*.
16. Schumacher, M.; Kelkel, M.; Dicato, M.; Diederich, M. Gold from the sea: marine compounds as inhibitors of the hallmarks of cancer. *Biotechnol. Adv.* **2011,** *29*, 531-47.
17. Malve, H. Exploring the ocean for new drug developments: Marine pharmacology. *J. Pharm. Bioallied Sci.* **2016,** *8*, 83-91.
18. Jimenez, P. C.; Wilke, D. V.; Costa-Lotufo, L. V. Marine drugs for cancer: surfacing biotechnological innovations from the oceans. *Clinics* **2018,** *73*, e482s.
19. Roberts, W. K.; Dekker, C. A. A convenient synthesis of arabinosylcytosine (cytosine arabinoside). *J. Org. Chem.* **1967,** *32*, 816-7.
20. Bergmann, W.; Feeney, R. J. CONTRIBUTIONS TO THE STUDY OF MARINE PRODUCTS. XXXII. THE NUCLEOSIDES OF SPONGES. I.1. *J. Org.* **1951,** *16*, 981-987.
21. Mayer, A. M.; Glaser, K. B.; Cuevas, C.; Jacobs, R. S.; Kem, W.; Little, R.

D.; McIntosh, J. M.; Newman, D. J.; Potts, B. C.; Shuster, D. E. The odyssey of marine pharmaceuticals: a current pipeline perspective. *Trends Pharmacol. Sci.* **2010,** *31*, 255-65.

22. Hollenbeak, K. H.; Schmitz, F. J. Aplysinopsin: antineoplastic tryptophan derivative from the marine sponge Verongia spengelii. *Lloydia* **1977,** *40*, 479-81.
23. Murata, M.; Miyagawa-Kohshima, K.; Nakanishi, K.; Naya, Y. Characterization of compounds that induce symbiosis between sea anemone and anemone fish. *Science* **1986,** *234*, 585-7.
24. Okuda, R. K.; Klein, D.; Kinnel, R. B.; Li, M.; Scheuer, P. J., Marine natural products: the past twenty years and beyond. In *Pure and Applied Chemistry*, 1982; Vol. 54, p 1907.
25. Bialonska, D.; Zjawiony, J. K. Aplysinopsins - Marine Indole Alkaloids: Chemistry, Bioactivity and Ecological Significance. *Mar. Drugs* **2009,** *7*, 166-183.
26. Gribble, G. W. The diversity of naturally occurring organobromine compounds. *Chem. Soc. Rev.* **1999,** *28*, 335-346.
27. Hu, J. F.; Schetz, J. A.; Kelly, M.; Peng, J. N.; Ang, K. K.; Flotow, H.; Leong, C. Y.; Ng, S. B.; Buss, A. D.; Wilkins, S. P.; Hamann, M. T. New antiinfective and human 5-HT2 receptor binding natural and semisynthetic compounds from the Jamaican sponge Smenospongia aurea. *J. Nat. Prod.* **2002,** *65*, 476-80.
28. Whitebread, S.; Hamon, J.; Bojanic, D.; Urban, L. Keynote review: in vitro safety pharmacology profiling: an essential tool for successful drug development. *Drug Discov. Today* **2005,** *10*, 1421-33.
29. Amagata, T.; Tanaka, M.; Yamada, T.; Doi, M.; Minoura, K.; Ohishi, H.; Yamori, T.; Numata, A. Variation in cytostatic constituents of a sponge-derived Gymnascella dankaliensis by manipulating the carbon source. *J. Nat. Prod.* **2007,** *70*, 1731-40.
30. Ellithey, M. S.; Lall, N.; Hussein, A. A.; Meyer, D. Cytotoxic, cytostatic and HIV-1 PR inhibitory activities of the soft coral Litophyton arboreum. *Mar. Drugs* **2013,** *11*, 4917-36.

31. Acikgoz, E.; Guven, U.; Duzagac, F.; Uslu, R.; Kara, M.; Soner, B. C.; Oktem, G. Enhanced G2/M Arrest, Caspase Related Apoptosis and Reduced E-Cadherin Dependent Intercellular Adhesion by Trabectedin in Prostate Cancer Stem Cells. *PLoS One* **2015,** *10*, e0141090.
32. Giam, M.; Huang, D. C. S.; Bouillet, P. BH3-only proteins and their roles in programmed cell death. *Oncogene* **2008,** *27*, S128-S136.
33. Ni Chonghaile, T.; Letai, A. Mimicking the BH3 domain to kill cancer cells. *Oncogene* **2008,** *27 Suppl 1*, S149-S157.
34. Chonghaile, T. N. BH3 mimetics: Weapons of cancer cell destruction. *Sci. Transl.* **2019,** *11*, eaaw5311.
35. Cerella, C.; Gaigneaux, A.; Mazumder, A.; Lee, J. Y.; Saland, E.; Radogna, F.; Farge, T.; Vergez, F.; Récher, C.; Sarry, J. E.; Kim, K. W.; Shin, H. Y.; Dicato, M.; Diederich, M. Bcl-2 protein family expression pattern determines synergistic pro-apoptotic effects of BH3 mimetics with hemisynthetic cardiac glycoside UNBS1450 in acute myeloid leukemia. *Leukemia* **2017,** *31*, 755-759.
36. Lee, J. Y.; Talhi, O.; Jang, D.; Cerella, C.; Gaigneaux, A.; Kim, K. W.; Lee, J. W.; Dicato, M.; Bachari, K.; Han, B. W.; Silva, A. M. S.; Orlikova, B.; Diederich, M. Cytostatic hydroxycoumarin OT52 induces ER/Golgi stress and STAT3 inhibition triggering non-canonical cell death and synergy with BH3 mimetics in lung cancer. *Cancer Lett.* **2018,** *416*, 94-108.

6. CONCLUSIONS

Through the screening of several aplysinopsin analogs, I selected EE-84 as an interesting anti-leukemic agent. EE-84 exhibited a safety profile as it had minimal impact on the healthy models *in vitro* and *in vivo*. I also found that the treatment of K562 with EE-84 induced anti-proliferative effect alongside dysfunction in the cell cycle progression. In addition, cellular stress was observed by examination of EE-84 treated K562 cells morphology. Treatment of EE-84 in combination with a BH3 mimetic A-1210477 showed an increase in apoptotic cell death potentializing the co-treatment as an alternate therapeutic approach to therapeutic failure of drugs already in the market. Figure 13 represents the overview of the results obtained.

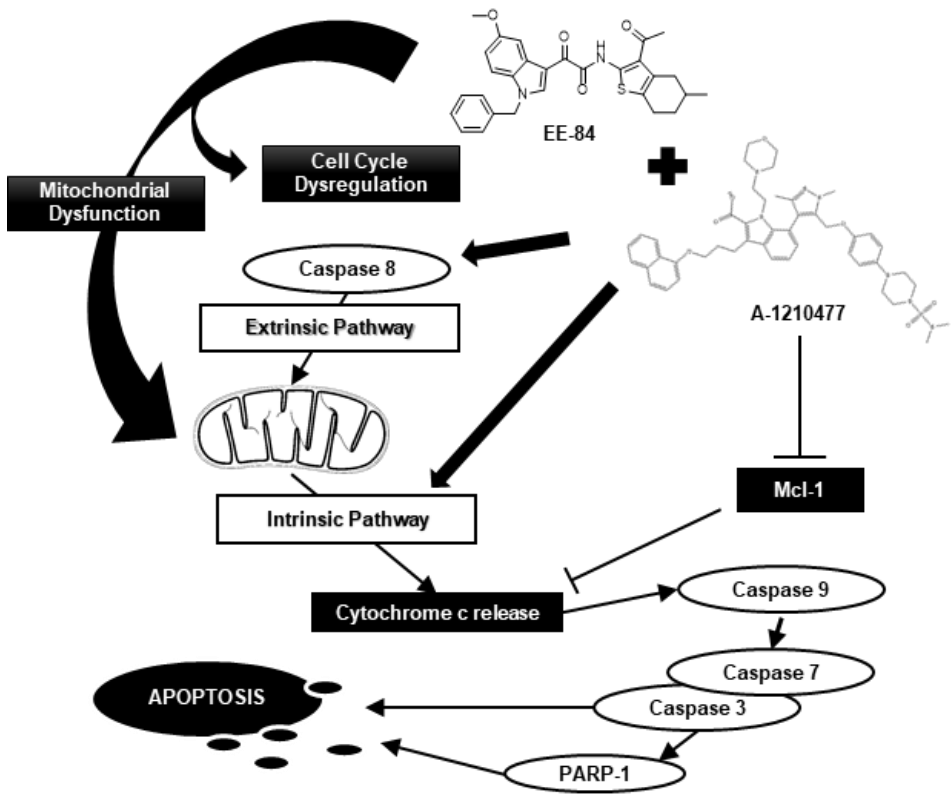

7. 국문초록

Aplysinopsin은 항암 효과와 같은 다양한 생물학적 활성을 나타내는 해양 인돌 알카로이드 계열의 천연화합물이다. Indole 및 N-benzyl moiety를 가진 aplysinopsin과 그의 유사체들은 암 세포에 대한 항 증식 활성을 갖는 것으로 알려졌지만, 이들의 작용 메커니즘은 아직 불명확하다. *In vitro* 독성 시험 – cell proliferation과 cell viability 분석 및 colony formation assay – 그리고 *in vivo* zebrafish toxicity test를 통해 백혈병 세포주에서의 aplysinopsin 화합물 치료 가능성을 확인한 결과, EE-84는 잠재적인 drug lead인 것을 나타냈다. EE-84은 Lipinski의 rule of five에 따라 약물 유사성을 보여주었고 이 인돌 유사체는 K562 세포에서 cell cycle dysfunction을 유도하였다. EE-84가 처리된 K562 세포들도 마찬가지로 형태변화를 겪는데 이는 시간 경과에 따른 cellular 스트레스를 암시한다. 결과적으로 본 연구에서 BH3 모방체와 함께 EE-84의 세포사멸 동반상승효과를 보였으며, K562 성장에 반하는 Mcl-1 억제제는 백혈병에 관해 유망한 치료적 접근으로서 anti-apoptotic machinery의 억제를 강조하였다.